Adeno-Associated Virus based Caveolin-1 Delivery via Different Routes for the Prevention of Cholesterol Gallstone Formation

Sha Li
Zhejiang University School of Medicine
Hongtan Chen
Zhejiang University School of Medicine
Xin Jiang
Zhejiang University School of Medicine
Fengling Hu
Zhejiang University School of Medicine
Yiqiao Li (yiqiao626@163.com)
Zhejiang Provincial People's Hospital and Hangzhou Medical College Affiliated People's Hospital
Guoqiang Xu
Zhejiang University School of Medicine

Research Article

Keywords: cholesterol gallstone disease, caveolin-1, adenosine monophosphate-activated protein kinase, mucin-1, mucin-5ac

Posted Date: July 25th, 2022

DOI: https://doi.org/10.21203/rs.3.rs-1852657/v1

Abstract

Background

The hepatic caveolin1 (CAV1) was reduced in cholesterol gallstone disease (CGD). And mice with CAV1 deficiency were prone to develop CGD. However, it remains unknown whether the restored hepatic CAV1 expression would prevent the development of CGD.

Methods

C57BL/6 mice were injected with adeno-associated virus 2/8 (AAV2/8) vectors carrying CAV1 gene ($^{AAV2/8}$CAV1) via intravenous (i.v.) or intraperitoneal (i.p.) route and then were subjected to a lithogenic diet (LD) for 8 weeks. Uninjected mice were used as control. The functional consequences of rescuing CAV1 expression by either i.v. or i.p. $^{AAV2/8}$CAV1 treatment on CGD prevention and its subsequent molecular mechanisms were examined.

Results

The CAV1 expression was reduced in liver and gallbladder of LD-fed-induced CGD mice. We discovered that $^{AAV2/8}$CAV1 i.p. delivery results in higher transduction efficiency in the gallbladder than tail vein administration. And although either i.v. or i.p. injection of $^{AAV2/8}$CAV1 improved the liver lipid metabolic abnormalities in CGD mice, they did not affect LD feeding-induced bile cholesterol supersaturation. In comparison with i.v. administration route, i.p. administration of $^{AAV2/8}$CAV1 obviously increased CAV1 protein levels in the gallbladder of LD-fed mice. And i.p. delivery of $^{AAV2/8}$CAV1 would partially improve gallbladder cholecystokinin receptor (CCKAR) responsiveness and impede bile cholesterol nucleation, via the activation of adenosine monophosphate-activated protein kinase (AMPK) signaling induced a reduction of gallbladder mucin-1 (MUC1) and MUC5ac expression and gallbladder cholesterol accumulation.

Conclusions

CGD prevention by i.p. $^{AAV2/8}$CAV1 injection in LD-fed mice was associated with the improvement of gallbladder stasis, which again supported the notion that supersaturated bile is required but not sufficient for the formation of cholesterol gallstones. Additionally, AAV treatment via local i.p. injection offers particular advantages over the systemic i.v. route for much more effective gallbladder gene delivery, which will be an excellent tool for conducting preclinical functional studies on the maintenance of normal gallbladder function to prevent CGD.

Introduction

Caveolae, which plays an important role in endocytosis and signal transduction, presents on the plasma membrane as a small, flask-shaped pit[1]. Caveolin-1 (CAV1) is an essential component of caveolae, which is also involved in vesicular trafficking, lipid and cholesterol metabolism and signal cascade[1]. CAV1 can traffic between the cytoplasm and membrane, contributing to the maintenance of intracellular cholesterol homeostasis and the transportation of extracellular cholesterol[2]. And intracellular cholesterol also affected caveolae density, CAV1 expression, and redistribution[2]. Despite CAV1 being distributed in both basolateral and apical plasma membranes of murine liver cells, caveolae only form in basolateral plasma membranes[3]. CAV1 can also be detected in endosomes, lipid droplets, mitochondria, endoplasmic reticulum, and other intracellular compartments, suggesting that CAV1 may act in a caveolae-independent manner in the liver[3]. CAV1 is believed to play a major role in cholesterol gallstone disease (CGD), nonalcoholic fatty liver disease (NAFLD), and other diseases associated with excessive cholesterol accumulation[2–6].

CGD are common. Although the exact molecular mechanism remains unclear, excessive accumulation of biliary cholesterol and abnormal cholesterol nucleation time (NT) are considered relevant factors for CGD development[7]. In the murine CGD model, we observed an increase in the secretion of biliary cholesterol, a decrease in the synthesis of bile acids, and an increase in bile cholesterol saturation index (CSI)[6]. Using CAV1 knockout mice can significantly increase the incidence of CGD after 4 weeks of lithogenetic diet[6]. However, it remains uncertain whether the overexpression of CAV1 will delay the formation of CGD.

The adeno-associated virus (AAV) is a member of the parvoviridae family, emerging as small, membraneless viruses with icosahedral structures[8]. These AAV constructs range in diameter from 20 to 26 nm and contain linear single-stranded DNA genomes ranging from 4.7 to 6 kb. AAV is widely acknowledged as a safe and effective form of gene delivery due to its low immunogenicity, high infection capacity, and long-term steady expression of genes. The systemic intravenous (i.v.) or local intraperitoneal (i.p.) injection of AAV-mediated gene delivery is a widely used approach for overexpression of a specific gene in the liver of mice [9]. However, it has been demonstrated before that i.p. injection of AAV transduces pancreatic cells more efficiently than i.v. injection [10, 11]. And is there a difference in gallbladder-directed AAV transduction efficiency between i.v. and i.p. routes? This question remains to be determined.

Through this study, we want to eluciate the effective method of gallbladder CAV1 overexpression via AVV gene delivery by comparing two different delivery routes (i.v. vs. i.p.). And the effects of CAV1 on the prevention of CGD should be investigated.

Material And Methods

Animals, diet and drug treatment

All animal experiments were conducted following the Chinese Ministry of Health national guidelines for the housing and care of laboratory animals and were approved by the Animal Committee of Zhejiang University (No. 2020 – 1288). Each mice experiment was performed in triplicate. 3-month-old male C57BL/6 mice (total number of mice = 84) were purchased from the Model Animal Research Center of Nanjing University (Nanjing, China). Numbers of mice/group were given in figure legends. All mice were housed in a pathogen-free animal facility under controlled conditions of humidity (55 ± 5%), lighting (12-hour light/dark cycle), and temperature (23°C), and were given diet and water *ad libitum*.

The murine CAV1 cDNA sequences were obtained from the PubMed database and were synthesized by Shanghai GeneChem Co., Ltd. (Shanghai, China), which then were cloned and packaged as AAV2 inverted terminal repeat DNA combined with the AAV8 capsid (AAV2/8) virus. To address the hypothesis that CAV1 gene overexpression by using AAV2/8 gene delivery ($^{AAV2/8}$CAV1) can prevent CGD, mice received a i.v. or i.p. injection of $^{AAV2/8}$CAV1 at a dose of 1×10^{11} viral genomes (vg)/animal, and were then fed a lithogenic diet (LD, TD.90221, containing 15.8% fat, 1.25% cholesterol, and 0.5% sodium cholate; Harlan Teklad Custom Research, Livermore, CA, USA), or a control chow diet (TD.2918; Harlan Teklad Custom Research, Livermore, CA, USA) for 8 weeks. Mice were then euthanized for collection of ileum, liver, and gallbladder tissues. Samples were snap frozen in liquid nitrogen and stored at − 80°C until analysis. For drug treatment, the adenosine monophosphate-activated protein kinase (AMPK) inhibitor compound c (866405-64-3, 10 mg/kg, i.p. injection once a day; Sigma, Ronkonkoma, NY, USA) was given at the beginning of the LD, and the drug treatments continued until the completion of the experiments.

Examination of AAV2/8CAV1 transduction efficiency

Frozen sections (5 μm thick) of the gallbladder, ileum, and liver from mice injected with or without $^{AAV2/8}$CAV1 (8 weeks post-injection) were used for immunoflorescence staining. Serial sections were incubated with the mixture of primary antibodies against CAV1 (Rabbit monoclonal, E249, 1:500; Abcam, UK) and βactin (mouse monoclonal 8226, 1:1000; Abcam, UK). After three washes, the mixture of secondary antibodies (cy3-conjugated goat anti-mouse IgG 2338714 and fluorescein isothiocyanate–conjugated goat anti–rabbit IgG 2337972; Jackson ImmunoResearch Laboratories) were overlaid. Cell nuclei were counterstained with 2-(4-Amidinophenyl)-6-indolecarbamidine (DAPI; 300 nM, D9542; Sigma, Ronkonkoma, NY, USA).

Fluorescent images of cryosection were recorded using an Olympus DP70 digital camera coupled to an Olympus IX71 inverted microscope (Tokyo, Japan). Fluorescence expression efficiency was measured using ImageJ software. The fluorescence intensities of CAV1 expression areas were normalized to the fluorescence intensities of βactin-stained areas. The double staining area of CAV1/βactin was counted in five different arbitrary areas from three independent experiments. Total intensities of 100 cells from multiple areas were accumulated and considered as the value of CAV1 and βactin expression in gallbladder, ileum, and liver from one mouse.

To investigate the efficiency of $^{AAV2/8}$CAV1 transduction, compared with the i.v. and i.p. routes, total DNA was extracted from the gallbladder, ileum and liver tissues of mice with a DNAeasy Blood and Tissue kit

(Qiagen 69504; Valencia, CA, USA) and vector genome copy number was determined with a 7900 HT real-time PCR system (Applied Biosystems; Foster City, CA, USA). TaqMan assays for viral vector genome copy number were developed using primers and probes for the AAV2/8 vector bearing a small chicken β-actin promoter region. Forward primer is 5'-TCTGCTTCACTCTCCCCATCTC-3'. Reverse primer is 5'-CCATCGCTGCACAAA- ATAATTAAA-3'. Fluorescent probe is 6-carboxyfluorescein-CCCCCTCCCCACCCCCAATT. The AAV2/8 vector genome copy number is normalized as viral genome copy number per μg of total genomic DNA.

LD consumption

After being fed the LD for 8 weeks, mice were singly housed. Food pellets were weighed (grams) per day in the morning over a 3-day LD consumption period and the amount of food left in the cages was subtracted from the initially recorded amount.

Measurement of fecal cholesterol excretion

After being fed the LD for 8 weeks, mice were singly housed. After a 3-day fecal collection, the mice were weighed, and the feces were dried in a 70°C vacuum oven, weighed, and crushed into a fine powder. A measured mass (50 mg) of feces was placed into a glass tube containing 103 μg of 5α-cholestane as an internal standard. The feces were saponified and the neutral lipids were extracted with hexane. Mass analysis of the extracted neutral sterols was conducted by the DIAN Diagnostics Laboratory (Hangzhou, China) using gas-liquid chromatography. Fecal cholesterol mass represents the sum of cholesterol and its derivatives (coprostanol and coprostanone) in each sample. Fecal cholesterol excretion was expressed as μmol/day/100 g body weight.

Biochemical analysis of liver and gallbladder tissues and gallbladder bile

After being fed LD for 8 weeks, the hepatic tissues (150 mg) of mice were homogenized, and the triglyceride, cholesterol, and free fatty acids (including palmitic, stearic, oleic, linoleic and arachidonic acid proportions) levels were examined by the DIAN Diagnostics Laboratory (Hangzhou, China).

The phospholipid, cholesterol and triglyceride levels in the gallbladder bile of 8-week LD-fed mice were measured by the DIAN Diagnostics Laboratory (Hangzhou, China). Total bile salts were quantified with the 3α-hydroxysteroid dehydrogenase enzymatic method. The cholesterol saturation index (CSI) was calculated according to Carey's critical table.

Microscopic examination of cholesterol crystals

After 8 weeks of LD, mice were fasted overnight and euthanized, then the intact gallbladders were harvested. Gallbladder bile was spread on glass slides and examined with a Leica DM5000 polarized microscope for the detection of cholesterol crystals.

Examination of gallbladder contraction

After being fed the LD for 8 weeks, the contractility of the gallbladder of mice was measured using a MyoMED myograph system (MED Associates, USA). Chow-fed mice were used as control. After anesthetized euthanasia, the gallbladders were removed and the gallbladder strips (measuring from 3 mm to 10 mm) were cut through the whole wall. The silk threads were attached to each end of the strips. Each strip was mounted in a tissue bath (15-mL volume) containing aerated (5% CO2/95% O2) physiological saline solution (containing 119 mM NaCl, 4.7 mM KCl, 24 mM NaHCO3, 1.2 mM KH2PO4, 2.5 mM CaCl2, 1.2 mM MgSO4, and 11 mM glucose; pH 7.4) at 37°C. These gallbladder strips were placed under an initial resting tension equivalent to a 5 mN load and allowed to equilibrate for 60 minutes, with solution changes every 15 minutes. Agonist responses were obtained by applying the neurotransmitter cholecystokinin (AS20741, 10 nM, AnaSpec, Fremont, USA) or the muscarinic agonist methacholine (carbachol 51-83-2, 0.1 ~ 30 μM, applied cumulatively; Sigma, Ronkonkoma, NY, USA) directly into the tissue bath. Responses were normalized to the wet weight of the tissue.

Quantitative real-time polymerase chain reaction (qRT-PCR) assays

The qRT-PCR was performed using total RNA extracted from ileum, liver, and gallbladder tissues of chow-fed and LD-fed mice (after 8-week feeding period). All used primer sequences were listed in Supplementary Table 1. Expression data were normalized to the expression of 18s RNA.

Western blot

The liver and gallbladder tissues collected from 8-week LD-fed mice were lysed with NE-PER™ nuclear and cytoplasmic extraction reagents (78833, ThermoFisher, Waltham, MA, USA) and complete protease inhibitor (11697498001, Roche, Basel, Switzerland) on ice. For immunoblot, the lysate proteins were resolved by SDS-PAGE and blotted onto nitrocellulose membranes to test the binding of the antibodies (The used antibodies were listed in Supplementary Table 2). Original data of western blot were shown in Supplementary Fig. 1–3.

Transfection of HepG2 cells and luciferase reporter assay

On Day 0, human liver HepG2 cells (HB-8065; ATCC, Manassas, VA, USA) were plated at density of 5 x 10^4 cells per well in 24-well plates in Eagle's Minimum Essential Medium (ThermoFisher, Waltham, MA, USA) supplemented with 10% fetal bovine serum (FBS; ThermoFisher, Waltham, MA, USA) and incubated at 37°C in a 5% CO_2 incubator. On Day 1, cells were washed with 0.5 ml phosphate-buffered saline (PBS) and 0.5 ml fresh Eagle's Minimum Essential Medium was added to each well before transfection. A 201 bp DNA fragment from intron 2 of human ATP binding cassette subfamily G member 5 (ABCG5) gene (Homo Sapiens Chr2, NC_000002.12: 43836293 ~ 43836093) [12], a 210 bp DNA fragment from intron 3 of human ATP binding cassette subfamily G member 8 (ABCG8) gene (Homo Sapiens Chr2, NC_000002.12: 43848694 ~ 43848903) [12], a 380 bp DNA fragment from the intragenic region of the human ABCG5/ABCG8 gene (Homo Sapiens Chr2, NC_000002.12: 443839056 ~ 43838677, in either the ABCG5 or ABCG8 orientation) [12] and a 420 bp DNA fragment from the fragment of the human sterol-regulatory-element-binding protein-1c (SREBP1c) promoter (Homo Sapiens Chr17, NC_000017.11:

17824067 ~ 17823648) [13] were synthesized by GenerayBiotech (GenerayBiotech, Shanghai, China) and were respectively inserted into a pGL3 firefly luciferase reporter vector (Promega, Madison, WI, USA). The pGL3 plasmid containing a 380 bp DNA fragment from the intragenic region of the human ABCG5/ABCG8 gene (in either the ABCG5 or ABCG8 orientation) served as a template to generate a GATA-mutated binding site (AGGCCG) construct, in which a putative GATA binding sites were (Homo Sapiens Chr2, NC_000017.11: 43838839 ~ 43838834; AGATAA) mutated [12]. Mutations were created by site-directed mutagenesis using the GeneArt™ Site-Directed Mutagenesis System (ThermoFisher A13282, Waltham, MA, USA). The mutation was sequence verified. Then HepG2 cells were, respectively, cotransfected with these above plasmids (0.25 μg) and a control plasmid pCMV-β-Gal vector (10 ng; Promega, Madison, WI, USA) containing the β-galactosidase reporter gene by using lipofectamine 2000 (ThermoFisher, Waltham, MA, USA) transfection reagent. Each transfection was done in triplicate wells. 6-hour after transfection, cells were washed with 0.5 ml PBS, switched with Eagle's Minimum Essential Medium supplemented with 10% FBS and 1 μM T0901317 (LXR agonist, Sigma, Ronkonkoma, NY, USA) plus 0.5 mM metformin (AMPK agonist, Sigma, Ronkonkoma, NY, USA), and incubated for 16 hours at 37°C and 5% CO_2. On Day 2, cells were washed with 0.5 ml PBS and firefly luciferase activities were measured using the Luciferase Assay System (Promega, Madison, WI, USA) and TD-20/20 Luminometer (Turner Designs, San Jose, CA, USA). β-galactosidae activity was measured by Galacto-Light β-Galactosidase Reporter Gene Assay System (ThermoFisher, Waltham, MA, USA). Firefly luciferase activities in the transfected lysates were normalized by β-galactosidase activity in the same tube.

Statistical analysis

Data are expressed as means ± standard deviation (SD). Statistical analysis was performed by using Prism (GraphPad Software, San Diego, CA, USA). Data normality was determined by using Shapiro-Wilkes test. The statistical analysis between two independent groups with normal distribution were determined by using Student's t-test, while Mann-Whitney test was used to compare non-normal data. For more than two normally distributed groups, statistical comparisons were made by one-way analysis of variance (ANOVA, equal variance between groups) or Welch's ANOVA (unequal variance between groups) with pairwise comparisons using Benjamini-Hochberg corrections. And Kruskal-Wallis nonparametric ANOVA with Benjamini-Hochberg correction was used to compare more than two samples with nonnormal distribution. $P < 0.05$ was considered significant.

Result

Intraperitoneal delivery leads to efficient gallbladder CAV1 gene transfer in mice.

Since CAV1 is widely distributed in the gallbladder, intestine, and liver tissues (https://www.proteinatlas.org/ENSG00000105974-CAV1/tissue), we evaluated the effect of different routes of delivery and AAV-mediated CAV1 gene transduction in those three tissues. We compared i.p. and i.v. $^{AAV2/8}$CAV1 delivery in adult mice. Briefly, 1×10^{11} vg per mice of the $^{AAV2/8}$CAV1 were administered to 8-week-old mice, either by i.v. or i.p. injection. 8-week post-injection, the liver, gallbladder, and ileum

tissues were collected to analyze CAV1 expression. No significant differences were observed in the CAV1 expression and the AAV vector genome copy number in the liver of mice between i.v. and i.p. injection (Figs. 1A **and B)**. And we found that i.p. $^{AAV2/8}$CAV1 delivery increased transduction efficiency in the gallbladder as compared with i.v. injection (Figs. 1A **and B)**. In addition, we confirmed that $^{AAV2/8}$CAV1 did not transduce in the ileum at high frequency (< 3% CAV1 gene transduction efficiency), which in consistent with prior findings [14]. Western blot further verified these above results (Fig. 1C**).**

Intraperitoneal administration of AAV2/8CAV1 prevent CGD, regardless changes of biliary CSI.

CAV1 is considered to participate in the regulation of hepatic lipid accumulation and cholesterol metabolism, thus playing an important role in the pathogenesis of diseases related to aberrant triglyceride or cholesterol metabolism[3]. Therefore, we examined the concentration of bile acid, lecithin, and cholesterol in gallbladder bile of chow-fed or LD-fed mice, after injection of $^{AAV2/8}$CAV1. 8-week LD feeding would reduce the hepatic and gallbladder CAV1 protein levels of control (uninjected) mice (Fig. 1C). Either i.v. or i.p. administration of $^{AAV2/8}$CAV1 would elevate the hepatic CAV1 expression collected from 8-week LD-fed mice (Fig. 1C). And CAV1 concentration in the gallbladder was higher in i.p. injected mice than in i.v. injected mice and control mice (Fig. 1C). CAV1 overexpression did not alter the feeding behavior of the mice (Fig. 2A). The intestinal expression of niemann-pick disease, type C1-like intracellular cholesterol transporter 1 (NPC1L1) and the fecal contents of cholesterol also were similar between control mice and $^{AAV2/8}$CAV1-treated mice after LD feeding (Fig. 2B **and C**), which implicated that CAV1 over-expression did not change oral cholesterol uptake.

CGD results from the imbalance between bile acids, cholesterol, and phospholipids in the gallbladder bile[4, 7]. The canalicular efflux of cholesterol, bile acids, and phospholipids is mediated by ABCG5/G8, bile salt export pump (BSEP), multidrug resistance protein 2 (MRP2) and multidrug resistance protein 2 (MDR2), respectively, which directly regulate bile cholesterol saturation, were similar between control mice and $^{AAV2/8}$CAV1 administered mice after LD feeding (Fig. 2B). There were no significant differences in the contents of biliary bile acids, cholesterol, phospholipids or biliary CSI between $^{AAV2/8}$CAV1-treated or control mice (Fig. 2D). However, the CGD prevalence (Fig. 2E) was similar between control (9/9) and i.v. $^{AAV2/8}$CAV1 treated mice after 8-week LD feeding (11/13), while which was detected as a lower incidence in LD-fed mice with i.p. $^{AAV2/8}$CAV1 administration (7/13).

AMPK transactivates ABCG5/G8 gene expression to increase biliary cholesterol output.

Our previous work has shown that global CAV1 deficiency would promote CGD via the progression of the dysfunction of hepatic lipid metabolism and the upregulation of liver X receptor (LXR)-ABCG5/G8 signaling [6]. Here we found that the hepatic triglyceride and cholesterol levels of LD-fed mice administered $^{AAV2/8}$CAV1 via either the i.v. or i.p. route were markedly reduced as compared with control mice (Fig. 3A).

This has borne out in several studies [15–19], and we have proved that CAV1 over-expression by $^{AAV2/8}$CAV1 treatment prevented LD feeding induced hepatic steatosis and abnormal lipid metabolism by reducing SREBP1c expression via AMPK pathway activation[20] (Fig. 3B). And AMPK also suppressed hepatic de novo cholesterol synthesis by inhibiting hepatic sterol-regulatory-element-binding protein-2 (SREBP2) maturation [20] (Fig. 3B), which may explain why hepatic cholesterol levels decreased but biliary cholesterol levels remained unchanged (Figs. 2D and 3A). And the treatment of compound c (AMPK inhibitor) removed the protective effects of $^{AAV2/8}$CAV1 treatment on aberrant hepatic lipid metabolism (Figs. 3A **and B)**. Additionally, hepatic principle bile acid synthesis enzyme cytochrome P450 7A1 (CYP7a1) expression was comparable between control mice and $^{AAV2/8}$CAV1-treated mice after LD feeding (Fig. 2B), although previous study has shown that AMPK limits the conversion of cholesterol to bile acids by suppressing the hepatic expression of the CYP7a1 in human HepG2 cells [21].

According to a large epidemiological work, AMPK may positively affect CGD via the transactivation of ABCG5/G8 [22]. And animal studies have shown that ABCG5/G8 plays a direct role in the process that leads to bile cholesterol supersaturation, which reduces hepatic cholesterol burden [23]. However, the hepatic cholesterol output and ABCG5/G8 expression remained unchanged between $^{AAV2/8}$CAV1-injected LD-fed mice, with or without compound c treatment (Figs. 2B, 2D). ABCG5/G8 genes have long been known as a direct target of the oxysterol receptors LXR [12]. Thus, four ABCG5/G8-LUC chimeric constructs were produced and transiently transfected into HepG2 cells to delineate the cis-acting regions of the ABCG5/G8 gene that are directly responsible for transcriptional regulation by LXR and AMPK. As predicted, the synthetic LXR ligand T0901317 compound (1 μM) would induce the expression of luciferase from reporters containing the potential LXR site [12] on ABCG5 gene intron 2 (5'-GGATCACTTGAGGTCA-3'; core similarity = 1.0, matrix similarity = 0.985) or on ABCG8 gene intron 3 (5'-GGATCACCTGAGGTCA-3'; core similarity = 1.0, matrix similarity = 0.935) (Fig. 4A), while this two DNA regions showed a reduced ability to respond to T0901317 in a reporter assay in the presence of AMPK activator (0.5 mM metformin). Furthermore, in consistent with previous reports[24], AMPK activation could impede LXR mediated SREBP1c gene transactivation (Fig. 4B).

Next, the luciferase activities of reports containing the 380 bp ABCG5/ABCG8 intergenic region induced by metformin (0.5 mM) in the absence or presence of T0901317 (1 μM) looked equal (Fig. 4C). Additionally, the report on the analysis of the human ABCG5/ABCG8 intergenic region for potential transcription factor binding sites revealed that there are only two regulatory elements, transcription enhancer factor 1 (TEF1) and GATA, that are present in in mouse and human species [12]. The presence of a GATA site (5'-AGATAA-3') is particularly interesting, because it is known to regulate the expression of ABCG5/G8 [25]. Indeed, AMPK could increase the DNA binding activity of GATA binding protein 4 (GATA4) [26]. And we performed a binding site mutagenesis combined with luciferase reporter assays to show that GATA site mutation impeded the role of AMPK on ABCG5/G8 gene transcription (Fig. 4D). These data implied that LXR and AMPK induced luciferase transactivation by acting on different sites of the ABCG5/G8 gene. And AMPK could suppress LXR-dependent ABCG5/G8 gene transcription.

Intraperitoneal AAV2/8CAV1 delivery prevents CGD via the reduction of gallbladder MUC1 expression and the improvement of gallbladder motility.

Unlike i.v. route, i.p. $^{AAV2/8}$CAV1 administration reduce CGD prevalence in LD-fed mice, although both of them did not affect LD feeding-induced bile cholesterol saturation (Figs. 2D **and E**). These data proved that bile cholesterol saturation is required but insufficient for CGD. The formation of cholesterol gallstones is also linked to the accumulation of pronucleating mucins in the gallbladder and its hypomotility, which would enhance the process of bile cholesterol nucleation [7]. It has been reported that epithelial mucin-1 (MUC1) could influence the gallbladder motility and the expression of pronucleating MUC5ac [27]. The gel-forming MUC5ac acted as a protective coating to accelerate the appearance of cholesterol monohydrate crystals, whereas mice with epithelial MUC1 deficiency were resistant to CGD due to decreased MUC5ac expression [28]. And only i.p. $^{AAV2/8}$CAV1 treatment lowered the gallbladder expression of MUC1 and MUC5ac ("MUC1,5ac") in LD-fed mice, which was attributed to CAV1-associated gallbladder AMPK activation initiating the microRNA-145 (miR145)/MUC1 axis [29, 30] and inhibiting epidermal growth factor receptor (EGFR)/MUC5ac signalling [31] **(**Fig. 5A **and B)**. And as expected, these effects on "MUC1,5ac" expression were significantly diminished following AMPK inhibition **(**Figs. 5A **and B)**.

Additionally, i.v. or i.p. $^{AAV2/8}$CAV1 injection rescued the diminished gallbladder smooth muscle contraction force in response to acetylcholine in LD-fed mice, while only i.p. $^{AAV2/8}$CAV1 administration having a mild effect on the damaged gallbladder motility in response to cholecystokinin **(**Fig. 5C**)**. The difference in gallbladder contraction force between acetylcholine and cholecystokinin stimulation could be a result of restored cholinergic receptor muscarinic 3 (CHRM3) expression in the gallbladder of LD-fed mice treated with $^{AAV2/8}$CAV1 treatment but who retained a down-regulated gallbladder cholecystokinin a receptor (CCKAR) expression **(**Fig. 5B**)**. And LD feeding or/and $^{AAV2/8}$CAV1 treatment did not affect gallbladder cholinergic receptor muscarinic 2 (CHRM2) expression **(**Fig. 5B**)**. Triglyceride-associated lipid stress contributes to muscarinic receptor damage [32], whereas excessive intracellular cholesterol accumulation impairs CCK signalling [7]. $^{AAV2/8}$CAV1 treatment could reduce gallbladder free fatty acid and triglyceride contents in 8-week LD-fed mice **(**Fig. 5D**)**, but only i.p. injection of $^{AAV2/8}$CAV1 would obviously diminish the cholesterol levels in the gallbladder cells **(**Fig. 5D**)**. However, the cholesterol content of the gallbladder was comparable between control and i.v. $^{AAV2/8}$CAV1-treated mice, possibly due to the increased gallbladder MUC1 expression of mice in response to LD feeding, who had a role in the gallbladder absorption of cholesterol from bile **(**Fig. 5A and 5B**)**. Notably, the expression of gallbladder NPC1L1 was similar between LD-fed mice, without or without $^{AAV2/8}$CAV1 treatment **(**Fig. 5B**)**. These findings suggested that the primary mechanism by which i.p. $^{AAV2/8}$CAV1 administration protects against CGD by preventing the hyperproduction of gallbladder MUC1.

Discussion

CGD occurs or recurs frequently, making it one of the most expensive gastrointestinal problems to treat [7]. While laparoscopic cholecystectomy is considered the gold standard for gallstone removal, bile duct injuries or long-term gastrointestinal abnormalities have been reported following surgery. Novel therapeutics are vigorously being sought to treat CGD. Laparoscopy combined with choledochoscopic lithotomy is a viable surgical option for CGD patients who still have normal gallbladder function [33]. However, CGD patients with gallbladder hypomotility might not be a good candidate for gallbladder preservation operation due to a high recurrence rate of gallstones. These data suggested that safeguarding gallbladder motility will aid in the development of novel CGD treatment strategies.

Previous work of Tharp et al. [34] using CGD mice found that maintaining gallbladder physiological function via gallbladder long-chain fatty acid transporter 2 (FATP2) deletion by the systemic i.v. injection of AAV-delivered short hairpin RNA (shRNA) is sufficient to prevent gallstone formation, even in the presence of supersaturated bile cholesterol. Here we found that the i.v. $^{AAV2/8}$CAV1 injection could elevated hepatic CAV1 expression in mice before or after the LD feeding. However, gallbadder CAV1 expression was marginally affected by $^{AAV2/8}$CAV1 treatment via i.v. route. The transgene sequence size may influence AAV transfer efficiency [35, 36], therefore the lower efficiency of AAV-assisted CAV1 gene delivery into the gallbladder tissues in our work compared with that of Tharp et al [34] might be attributed to the size of CAV1 gene coding sequence (CDS) is significantly higher than that of shRNA targeting FATP2. It has been described that local AAV delivery method such as i.p. injection is more efficient than systemic i.v. administration [11]. And we observed that $^{AAV2/8}$CAV1 injection via i.p. route led to an enhanced transduction efficiency in the gallbladder collected from chow-fed or 8-week LD-fed CGD mice compared to i.v. route, while hepatic CAV1 protein expression levels were similar between mice with i.p. or i.v. $^{AAV2/8}$CAV1 delivery. In addition, a minor change of CAV1 expression in the intestine of mice with either i.p. or i.v. $^{AAV2/8}$CAV1 treatment, which also similar to previous report [14].

We previously demonstrated that mice with global CAV1 knockout were prone to develop CGD [34]. In this work, an obvious CAV1 overexpression observed in the liver via i.v. $^{AAV2/8}$CAV1 treatment or in both the liver and the gallbladder through i.p. $^{AAV2/8}$CAV1 injection allow us to distinguish the role of CAV1 on gallbladder motility and its contribution to the prevention of CGD, independent of changes in bile cholesterol saturation. Either i.v. or i.p. $^{AAV2/8}$CAV1 injection would reduce LD-fed induced hepatic triglyceride and cholesterol accumulation via the increase of CAV1 protein levels. A potential mechanism for the alleviation of hepatic lipid abnormalities in LD-fed mice following $^{AAV2/8}$CAV1 treatment is associated with CAV1-mediated AMPK activation to down-regulate SREBP1c and SREBP2 [20, 24]. We also found that AMPK activation impeded LXR-ABCG5/G8, but it itself would increase ABCG5/G8 expression in the liver to promote cholesterol entering the bile, which would prevent liver cholesterol accumulation to alleviate LD-induced liver lipid toxicity. And we noticed that, unlike stimulation by LXR via intron bindings [12], AMPK-mediated ABCG5/G8 gene transactivity may be depending on a conservative GATA site in the intergenic region between the two genes [12, 26]. However, hepatic AMPK-ABCG5/G8 signaling activation also elevated the biliary CSI to increase CGD risk, that might be why LD-fed mice with or without $^{AAV2/8}$CAV1 injection exhibited a similar elevated biliary CSI.

The major difference between LD-fed mice with i.v. and i.p. $^{AAV2/8}$CAV1 delivery was the obviously CAV1-associated gallbladder AMPK activation and LD-induced gallbladder dysmotility. The expression of epithelial MUC1 and the gel-forming MUC5ac, which have been identified as the predominant pro-nucleating factors for CGD [27, 28, 31], also were down-regulated in LD-fed mice following i.p. injection of $^{AAV2/8}$CAV1. Gallbladder hypersecretion of "MUC1,5ac" and its abnormal emptying are two independent risk factors for gallbladder stasis and CGD [7]. However, mice transgenic for the human MUC1 gene displayed increased MUC5ac production and impairing gallbladder emptying function via increased gallbladder cholesterol absorption in response to LD, which implied that MUC1 provides a bridge between gallbladder hypomotility and pronucleating MUC5ac hyper-production [27]. Gallbladder AMPK activation induced by i.p. $^{AAV2/8}$CAV1 injection was responsible for the reduction of “MUC1,5ac” expression. And miR145, a downstream effector of AMPK signalling [37], could bind to the 3' untranslated region of the MUC1 gene [29, 30], thereby linking the reduction of MUC1 with AMPK signalling. Furthermore, it is well known that epithelial MUC1 on the cell surface promotes EGFR activation [38] and and that the epidermal growth factor (EGF)/EGFR axis induces MUC5AC expression [31], whereas AMPK inhibits EGFR activity [39]. Our experimental data proved that i.p. $^{AAV2/8}$CAV1 injection induced gallbladder AMPK activation and MUC5ac expression downregulation, which might be via modulating EGFR phosphorylation. However, whether i.p. $^{AAV2/8}$CAV1 injection induced gallbladder MUC1 reduction contributing to AMPK-mediated downregulation of EGFR/MUC5ac signalling remains unknown.

Furthermore, meal-stimulated gallbladder emptying occurs as a result of gallbladder contraction mediated by CCK and/or acetylcholine signalling [40], which, when weakened by gallbladder lipid accumulation due to LD, may provide the retention time for bile cholesterol nucleation [7]. Acetylcholine contracts the gallbladder through CHRM2 and 3 [41], while CCK regulates gallbladder motility via CCKAR [7]. CHRM3 and CCKAR expression in the gallbladder of LD-fed mice was lowered, while CHRM2 expression was unaffected. Here, by using LD-fed mice, we found that either i.v. or i.p. $^{AAV2/8}$CAV1 delivery could improve gallbladder cholinergic responsiveness, which might be attributed to a restored gallbladder CHRM3 expression by the hepatic CAV1/AMPK axis contributing to the whole body lipid homeostasis. However, only i.p. $^{AAV2/8}$CAV1 aministration partially repaired the responsiveness of gallbladder to CCK, but neither it nor i.v. $^{AAV2/8}$CAV1 aministration had any influence on the reduced CCKAR or on the increased NPC1L1 in the gallbladder of LD-fed mice. The work of Wang et al. [27] provides evidence that MUC1 increases gallbladder cholesterol uptake from supersaturated bile and impairs its motility. And cholesterol accumulation would decouple phospholipase C signaling from CCKAR, thereby impairing the physiological gallbladder motility [7]. In addition, gallbladder cells do not have the ability to assemble lipoproteins and transport them into plasma [27]. Therefore, the discrepancy in gallbladder CCK responsiveness between i.v. and i.p. $^{AAV2/8}$CAV1 treatment was attributable to the i.p. route of $^{AAV2/8}$CAV1 injection inhibiting MUC1-related gallbladder cholesterol absorption from the bile via the gallbladder CAV1/AMPK axis. And further work elucidating the underlying mechanisms of LD feeding on the reduced expression of CHRM3 and CCKAR in the gallbladder may support advancements in the prevention and treatment of CGD.

Conclusions

In summary, these data might lead to the conclusion that CGD prevention by i.p. $^{AAV2/8}$CAV1 injection via the improvement of gallbladder stasis was relied on the activation of gallbladder AMPK signaling. And our study showed that AAV treatment via local i.p. injection offers particular advantages over the systemic i.v. route for much more effective gallbladder gene delivery, which will be an excellent tool for conducting preclinical functional studies on the maintenance of normal gallbladder function to prevent CGD.

List Of Abbreviations

DAPI, 2-(4-Amidinophenyl)-6-indolecarbamidine; AAV2/8, AAV2 inverted terminal repeat DNA combined with the AAV8 capsid; AAV, adeno-associated virus; AMPK, adenosine monophosphate-activated protein kinase; ABCG5, ATP binding cassette subfamily G member 5; BSEP, bile salt export pump; CAV1, caveolin-1; CGD, cholesterol gallstone disease; CSI, cholesterol saturation index; CHRM2, cholinergic receptor muscarinic 3; CHRM3, cholinergic receptor muscarinic 3; CDS, coding sequence; CYP7a1, cytochrome P450 7A1; EGFR, epidermal growth factor receptor; EGF, epidermal growth factor; GATA4, GATA binding protein 4; i.v., intravenous; LD, lithogenic diet; LXR, liver X receptor; i.p., local intraperitoneal; miR145, microRNA-145; MUC1, mucin-1; MUC5ac, mucin-5ac; MDR2, multidrug resistance protein 2; MRP2, multidrug resistance protein 2; type C1-like intracellular cholesterol transporter 1, niemann-pick disease; NAFLD, nonalcoholic fatty liver disease; NT, nucleation time; SREBP1c, sterol-regulatory-element-binding protein-1c; SREBP2, sterol-regulatory-element-binding protein-2; TEF1, transcription enhancer factor 1; vg, viral genomes

Declarations

Ethics approval and consent to participate

All animal experiments were conducted following the Chinese Ministry of Health national guidelines for the housing and care of laboratory animals and were approved by the Animal Committee of Zhejiang University (No. 2020-1288).

Consent for publication

All listed authors have approved the manuscript before submission.

Availability of data and materials

The data that support the findings of this study are available in the supplementary data in this article.

Competing interests

The authors do not have any disclosures to report.

Funding

This work was supported by National Natural Science Foundation of China (grant numbers 81870433 and 82170649) and Basic Public Welfare Research Program of Zhejiang Province (grant number LGJ18H030001).

Authors' contributions

Yiqiao Li and Guoqiang Xu designed the experiments. Sha Li, Hongtan Chen, Fengling Hu, Yiqiao Li performed the experiments. Xin Jiang and Yiqiao Li analyzed data. Yiqiao Li and and Guoqiang Xu wrote the manuscript. Guoqiang Xu supervised the project.

Acknowledgements

No applicable.

Authors' information (optional)

Ph.D. Sha Li, Ph.D. Hongtan Chen, Ph.D. Xin Jiang, M.D. Fengling Hu and M.D. Guoqiang Xu

Department of Gastroenterology

The First Affiliated Hospital, Zhejiang University School of Medicine

79 Qingchun Road

Hangzhou, Zhejiang, 310006, China

M.D. Yiqiao Li

Urology& Nephrology Center, Department of Nephrology

Zhejiang Provincial People's Hospital and Hangzhou Medical College Affiliated People's Hospital

158 Shangtang Road

Hangzhou 310014, Zhejiang, China.

References

1. Parton RG, del Pozo MA: **Caveolae as plasma membrane sensors, protectors and organizers**. Nat Rev Mol Cell Biol 2013, **14**:98–112.
2. Sohn J, Lin H, Fritch MR, Tuan RS: **Influence of cholesterol/caveolin-1/caveolae homeostasis on membrane properties and substrate adhesion characteristics of adult human mesenchymal stem cells**. Stem Cell Res Ther 2018, **9**:86.

3. Fernandez-Rojo MA, Ramm GA: **Caveolin-1 Function in Liver Physiology and Disease**. Trends Mol Med 2016, **22**:889–904.
4. Hernandez-Nazara A, Curiel-Lopez F, Martinez-Lopez E, Hernandez-Nazara Z, Panduro A: **Genetic predisposition of cholesterol gallstone disease**. Ann Hepatol 2006, **5**:140–149.
5. Bosch M, Mari M, Herms A, Fernandez A, Fajardo A, Kassan A, Giralt A, Colell A, Balgoma D, Barbero E, et al: **Caveolin-1 deficiency causes cholesterol-dependent mitochondrial dysfunction and apoptotic susceptibility**. Curr Biol 2011, **21**:681–686.
6. Xu G, Li Y, Jiang X, Chen H: **CAV1 Prevents Gallbladder Cholesterol Crystallization by Regulating Biosynthesis and Transport of Bile Salts**. J Cell Biochem 2016, **117**:2118–2127.
7. Di Ciaula A, Wang DQ, Portincasa P: **An update on the pathogenesis of cholesterol gallstone disease**. Curr Opin Gastroenterol 2018, **34**:71–80.
8. Riyad JM, Weber T: **Intracellular trafficking of adeno-associated virus (AAV) vectors: challenges and future directions**. Gene Ther 2021, **28**:683–696.
9. Dane AP, Wowro SJ, Cunningham SC, Alexander IE: **Comparison of gene transfer to the murine liver following intraperitoneal and intraportal delivery of hepatotropic AAV pseudo-serotypes**. Gene Ther 2013, **20**:460–464.
10. Ramzy A, Tuduri E, Glavas MM, Baker RK, Mojibian M, Fox JK, O'Dwyer SM, Dai D, Hu X, Denroche HC, et al: **AAV8 Ins1-Cre can produce efficient beta-cell recombination but requires consideration of off-target effects**. Sci Rep 2020, **10**:10518.
11. Chen M, Maeng K, Nawab A, Francois RA, Bray JK, Reinhard MK, Boye SL, Hauswirth WW, Kaye FJ, Aslanidi G, et al: **Efficient Gene Delivery and Expression in Pancreas and Pancreatic Tumors by Capsid-Optimized AAV8 Vectors**. Hum Gene Ther Methods 2017, **28**:49–59.
12. Remaley AT, Bark S, Walts AD, Freeman L, Shulenin S, Annilo T, Elgin E, Rhodes HE, Joyce C, Dean M, et al: **Comparative genome analysis of potential regulatory elements in the ABCG5-ABCG8 gene cluster**. Biochem Biophys Res Commun 2002, **295**:276–282.
13. Dif N, Euthine V, Gonnet E, Laville M, Vidal H, Lefai E: **Insulin activates human sterol-regulatory-element-binding protein-1c (SREBP-1c) promoter through SRE motifs**. Biochem J 2006, **400**:179–188.
14. Polyak S, Mah C, Porvasnik S, Herlihy JD, Campbell-Thompson M, Byrne BJ, Valentine JF: **Gene delivery to intestinal epithelial cells in vitro and in vivo with recombinant adeno-associated virus types 1, 2 and 5**. *Dig Dis Sci* 2008, **53**:1261–1270.
15. Wang J, Jiang W, Xin J, Xue W, Shi C, Wen J, Huang Y, Hu C: **Caveolin-1 Alleviates Acetaminophen-Induced Fat Accumulation in Non-Alcoholic Fatty Liver Disease by Enhancing Hepatic Antioxidant Ability via Activating AMPK Pathway**. Front Pharmacol 2021, **12**:717276.
16. Zhang Q, Wang J, Li H, Zhang Y, Chu X, Yang J, Li Y: **LncRNA Gm12664-001 ameliorates nonalcoholic fatty liver through modulating miR-295-5p and CAV1 expression**. Nutr Metab (Lond) 2020, **17**:13.

17. Han M, Pioronska W, Wang S, Nwosu ZC, Sticht C, Wang S, Gao Y, Ebert MP, Dooley S, Meyer C: **Hepatocyte caveolin-1 modulates metabolic gene profiles and functions in non-alcoholic fatty liver disease**. Cell Death Dis 2020, **11**:104.
18. Xue W, Wang J, Jiang W, Shi C, Wang X, Huang Y, Hu C: **Caveolin-1 alleviates lipid accumulation in NAFLD associated with promoting autophagy by inhibiting the Akt/mTOR pathway**. Eur J Pharmacol 2020, **871**:172910.
19. Li M, Chen D, Huang H, Wang J, Wan X, Xu C, Li C, Ma H, Yu C, Li Y: **Caveolin1 protects against diet induced hepatic lipid accumulation in mice**. PLoS One 2017, **12**:e0178748.
20. Li Y, Xu S, Mihaylova MM, Zheng B, Hou X, Jiang B, Park O, Luo Z, Lefai E, Shyy JY, et al: **AMPK phosphorylates and inhibits SREBP activity to attenuate hepatic steatosis and atherosclerosis in diet-induced insulin-resistant mice**. Cell Metab 2011, **13**:376–388.
21. Li T, Chanda D, Zhang Y, Choi HS, Chiang JY: **Glucose stimulates cholesterol 7alpha-hydroxylase gene transcription in human hepatocytes**. J Lipid Res 2010, **51**:832–842.
22. Sun D, Niu Z, Zheng HX, Wu F, Jiang L, Han TQ, Wei Y, Wang J, Jin L: **A Mitochondrial DNA Variant Elevates the Risk of Gallstone Disease by Altering Mitochondrial Function**. Cell Mol Gastroenterol Hepatol 2021, **11**:1211–1226 e1215.
23. Zein AA, Kaur R, Hussein TOK, Graf GA, Lee JY: **ABCG5/G8: a structural view to pathophysiology of the hepatobiliary cholesterol secretion**. Biochem Soc Trans 2019, **47**:1259–1268.
24. Yap F, Craddock L, Yang J: **Mechanism of AMPK suppression of LXR-dependent Srebp-1c transcription**. Int J Biol Sci 2011, **7**:645–650.
25. Sumi K, Tanaka T, Uchida A, Magoori K, Urashima Y, Ohashi R, Ohguchi H, Okamura M, Kudo H, Daigo K, et al: **Cooperative interaction between hepatocyte nuclear factor 4 alpha and GATA transcription factors regulates ATP-binding cassette sterol transporters ABCG5 and ABCG8**. Mol Cell Biol 2007, **27**:4248–4260.
26. Irrcher I, Ljubicic V, Kirwan AF, Hood DA: **AMP-activated protein kinase-regulated activation of the PGC-1alpha promoter in skeletal muscle cells**. PLoS One 2008, **3**:e3614.
27. Wang HH, Afdhal NH, Gendler SJ, Wang DQ: **Evidence that gallbladder epithelial mucin enhances cholesterol cholelithogenesis in MUC1 transgenic mice**. Gastroenterology 2006, **131**:210–222.
28. Wang HH, Afdhal NH, Gendler SJ, Wang DQ: **Targeted disruption of the murine mucin gene 1 decreases susceptibility to cholesterol gallstone formation**. J Lipid Res 2004, **45**:438–447.
29. Sachdeva M, Mo YY: **MicroRNA-145 suppresses cell invasion and metastasis by directly targeting mucin 1**. Cancer Res 2010, **70**:378–387.
30. Jara D, Carvajal P, Castro I, Barrera MJ, Aguilera S, Gonzalez S, Molina C, Hermoso M, Gonzalez MJ: **Type I Interferon Dependent hsa-miR-145-5p Downregulation Modulates MUC1 and TLR4 Overexpression in Salivary Glands From Sjogren's Syndrome Patients**. Front Immunol 2021, **12**:685837.
31. Finzi L, Barbu V, Burgel PR, Mergey M, Kirkwood KS, Wick EC, Scoazec JY, Peschaud F, Paye F, Nadel JA, Housset C: **MUC5AC, a gel-forming mucin accumulating in gallstone disease, is overproduced via**

an epidermal growth factor receptor pathway in the human gallbladder. Am J Pathol 2006, **169**:2031–2041.

32. Blanc EM, Kelly JF, Mark RJ, Waeg G, Mattson MP: **4-Hydroxynonenal, an aldehydic product of lipid peroxidation, impairs signal transduction associated with muscarinic acetylcholine and metabotropic glutamate receptors: possible action on G alpha(q/11)**. J Neurochem 1997, **69**:570–580.
33. Wang B, Huang A, Jiang M, Li H, Bao W, Ding K, Jiang Z, Zhao G, Hu H: **Risk Factors for Early Recurrence of Gallstones in Patients Undergoing Laparoscopy Combined With Choledochoscopic Lithotomy: A Single-Center Prospective Study**. Front Surg 2021, **8**:759390.
34. Tharp KM, Khalifeh-Soltani A, Park HM, Yurek DA, Falcon A, Wong L, Feng R, Atabai K, Stahl A: **Prevention of gallbladder hypomotility via FATP2 inhibition protects from lithogenic diet-induced cholelithiasis**. Am J Physiol Gastrointest Liver Physiol 2016, **310**:G855-864.
35. Maurer AC, Weitzman MD: **Adeno-Associated Virus Genome Interactions Important for Vector Production and Transduction**. Hum Gene Ther 2020, **31**:499–511.
36. Grieger JC, Samulski RJ: **Packaging capacity of adeno-associated virus serotypes: impact of larger genomes on infectivity and postentry steps**. J Virol 2005, **79**:9933–9944.
37. Kohlstedt K, Trouvain C, Boettger T, Shi L, Fisslthaler B, Fleming I: **AMP-activated protein kinase regulates endothelial cell angiotensin-converting enzyme expression via p53 and the post-transcriptional regulation of microRNA-143/145**. Circ Res 2013, **112**:1150–1158.
38. Schroeder JA, Thompson MC, Gardner MM, Gendler SJ: **Transgenic MUC1 interacts with epidermal growth factor receptor and correlates with mitogen-activated protein kinase activation in the mouse mammary gland**. J Biol Chem 2001, **276**:13057–13064.
39. Jhaveri TZ, Woo J, Shang X, Park BH, Gabrielson E: **AMP-activated kinase (AMPK) regulates activity of HER2 and EGFR in breast cancer**. Oncotarget 2015, **6**:14754–14765.
40. Mawe GM: **Nerves and Hormones Interact to Control Gallbladder Function**. News Physiol Sci 1998, **13**:84–90.
41. Tanahashi Y, Komori S, Matsuyama H, Kitazawa T, Unno T: **Functions of Muscarinic Receptor Subtypes in Gastrointestinal Smooth Muscle: A Review of Studies with Receptor-Knockout Mice**. Int J Mol Sci 2021, **22**.

Figures

Figure 1

The i.p. injection improves the delivery of $^{AAV2/8}$CAV1 to mice gallbladder compare with i.v. injection.

Mice were injected (either via i.v. or i.p.) with or without $^{AAV2/8}$CAV1 at 1×10^{11} vg/animal, and then assigned to chow or LD (8-week). Data with different lowercase letters indicates significant difference. The individual *P* values were described in Supplementary Table 3.

A. Serial sections of frozen (5 μm) liver, gallbladder, and ileum tissues collected from mice were stained for βactin (red) to quantify cell-specific CAV1 (green) transduction percentages. Representative images are shown. Blue: DAPI staining for nuclei. Scale bar: 100 μm. Quantification of liver, gallbladder, and ileum transduction was determined by the percentage of CAV1 staining-positive area. Results in the lower panel are shown as the mean ± SD (three sections from each animal were analyzed). n = 13 each group, mice with either i.v. or i.p. administration of $^{AAV2/8}$CAV1; n = 5 for control (uninjected) mice.

B. qRT-PCR analysis of AAV genomes in liver, gallbladder, and ileum collected from chow-fed (n = 9 each group, mice with either i.v. or i.p. administration of $^{AAV2/8}$CAV1) or LD-fed (n = 13 each group, mice with either i.v. or i.p. administration of $^{AAV2/8}$CAV1) mice.

C. western blot analysis of CAV1 protein expression in the liver, gallbladder, and ileum of chow-fed or LD-fed mice. βactin was used as a loading control. Data are representative of three samples for each protein. i.v., $^{AAV2/8}$CAV1 injection (1×10^{11} vg/mice) via i.v. route; i.p., $^{AAV2/8}$CAV1 injection (1×10^{11} vg/mice) via i.p. route.

D. western blot analysis for the comparison of CAV1 protein expression in the gallbladder of chow-fed or LD-fed mice between i.v. (1×10^{11} vg/mice) and i.p. (1×10^{11} vg/mice) routes of administration of $^{AAV2/8}$CAV1. βactin was used as a loading control. Data are representative of three samples for each protein.

Figure 2

$^{AAV2/8}$CAV1 treatment via the i.p. route can partially prevented CGD in LD-fed mice through the biliary CSI-independent pathway.

Mice were injected (either via i.v. or i.p.) with or without $^{AAV2/8}$CAV1 at 1×10^{11} vg/animal, and then fed LD following PBS or compound c treatment (8-week). n = 13 each group, LD-fed mice with either i.v. or i.p. administration of $^{AAV2/8}$CAV1, and with or without compound c treatment (10 mg/kg, i.p. injection once a day); n = 9 for LD-fed mice (control) with neither $^{AAV2/8}$CAV1 administration nor compound c treatment.

Data with different lowercase letters indicates significant difference. The individual *P* values were described in Supplementary Table 3.

A. lithogenic diet mass consumed in each group mouse.

B. qRT-PCR analysis of the liver, gallbladder, and ileum messenger RNA expression of cholesterol, phospholipid transporters, and bile acid transporters in each group mice. 18S rRNA was used as an internal control. Data represent mean ± SD.

C. 24-hour cumulative feces samples collected from each group mice were pooled and measured for total cholesterol contents.

D. biliary concentrations of cholesterol, phospholipids, bile acid, and CSI in each group mouse.

E. polarizing light microscopy examination of cholesterol crystals in the gallbladder of each group mouse. i.v., $^{AAV2/8}$CAV1 injection (1×10^{11} vg/mice) via i.v. route; i.p., $^{AAV2/8}$CAV1 injection (1×10^{11} vg/mice) via i.p. route.

Figure 3

AMPK inhibition hampered the protection of $^{AAV2/8}$CAV1 treatment on LD-induced hepatic lipid accumulation.

Mice were injected (either via i.v. or i.p.) with or without $^{AAV2/8}$CAV1 at 1×10^{11} vg/animal, and then fed LD. n = 13 each group, LD-fed mice with either i.v. or i.p. administration of $^{AAV2/8}$CAV1, and with or without compound c treatment (10 mg/kg, i.p. injection once a day); n = 9 for LD-fed mice (control) with neither $^{AAV2/8}$CAV1 administration nor compound c treatment.

Data with different lowercase letters indicates significant difference. The individual *P* values were described in Supplementary Table 3.

A. Quantitation of free fatty acids, triacylglycerol, and cholesterol in the liver of each group mice.

B. Proportion of each liver free fatty acid profile (palmitic acid, stearic acid, oleic acid, linoleic acid, and arachidonic acid) in each group mouse.

C. western blot analysis of AMPK (and its phosphorylation), CAV1, and SREBP1c protein expression in the liver and gallbladder of each group mouse. βactin was used as a loading control. Data are representative of three samples for each protein. T172, the activation marker of AMPK phosphorylation at threonine 172; i.v., $^{AAV2/8}$CAV1 injection (1×10^{11} vg/mice) via i.v. route; i.p., $^{AAV2/8}$CAV1 injection (1×10^{11} vg/mice) via i.p. route; CC, compound C injection (10 mg/kg/day) via i.p. route.

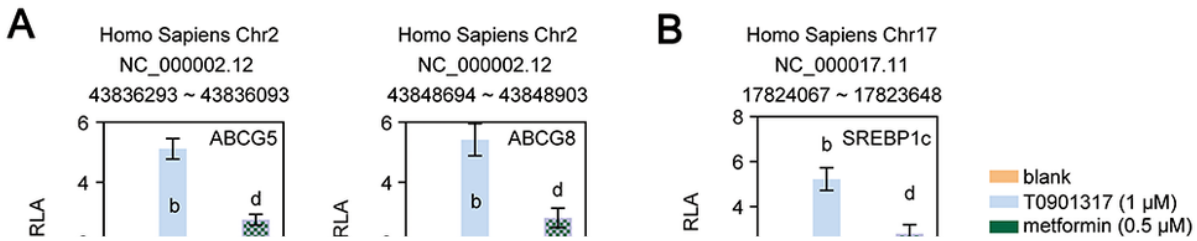

Figure 4

AMPK and LXR transactivate the human ABCG5/G8 gene at different sites.

Data represent mean ± SD of fold-independent experiments, expressed as fold-change vs. untreated cells.

Data with different lowercase letters indicates significant difference. The individual *P* values were described in Supplementary Table 3.

RLA, relative luciferase activity.

A and B. HepG2 cells were cotransfected with the pGL3 reporter containing containing a DNA fragment from intron 2 of the human ABCG5 gene (A left panel), or a DNA fragment from intron 3 of human ABCG8 gene (A, right panel), or an intragenic region (in either the ABCG5 or ABCG8 orientation) of the human ABCG5/ABCG8 gene (B), and a control plasmid (the plasmid containing the β-galactosidase reporter gene). Six hours after transfection, cells were treated with 1 μM T0901317 (LXR agonist) plus 0.5 mM metformin (AMPK agonist). Untreated cells were used as control. 24-hour later, cells were washed with 0.5 mL PBS, and luciferase and β-galactosidase activities were quantified using a luciferase assay kit. Normalized firefly luciferase activity by β-galactosidase activity without treatment was set as 1.

C. HepG2 cells were cotransfected with the pGL3 reporter containing a 420 bp DNA fragment from the fragment of the human SREBP1c promoter and a control plasmid (the plasmid containing the β-galactosidase reporter gene). Six hours after transfection, cells were treated with 1 μM T0901317 (LXR

agonist) plus 0.5 mM metformin (AMPK agonist). Untreated cells were used as control. 24 hours later, cells were washed with 0.5 mL PBS, and luciferase and β-galactosidase activities were quantified using a luciferase assay kit. Normalized firefly luciferase activity by β-galactosidase activity without treatment was set as 1.

D. HepG2 cells were cotransfected with the pGL3 reporter containing an intragenic region of the human ABCG5/ABCG8 gene (in either the ABCG5 or ABCG8 orientation) with a GATA-mutated binding site, or a wild type intragenic region of the human ABCG5/ABCG8 gene (in either the ABCG5 or ABCG8 orientation), and a control plasmid (the plasmid containing the β-galactosidase reporter gene). Six hours after transfection, cells were treated with 0.5 mM metformin (AMPK agonist) or plus 1 μM T0901317 (LXR agonist). Untreated cells were used as control. 24 hours later, cells were washed with 0.5 mL PBS, and luciferase and β-galactosidase activities were quantified using a luciferase assay kit. Normalized firefly luciferase activity by β-galactosidase activity without treatment was set as 1. WT, wild type; mutated, GATA binding site mutation; underlying uppercase letter, GATA binding sequence; uppercase letter in red, mutated GATA binding sequence.

Figure 5

CAV1-associated gallbladder AMPK activation protects mice from LD-induced CGD via the prevention of gallbladder stasis.

Mice were injected (either via i.v. or i.p.) with or without $^{AAV2/8}$CAV1 at 1×10^{11} vg/animal, and then fed LD following PBS or compound c treatment (8-week). n = 13 each group, LD-fed mice with either i.v. or i.p. administration of $^{AAV2/8}$CAV1, and with or without compound c treatment (10 mg/kg, i.p. injection once a day); n = 9 for LD-fed mice with neither $^{AAV2/8}$CAV1 administration nor compound c treatment. Chow-fed mice (8-week, n = 5) were used as control.

Data with different lowercase letters indicates significant difference. The individual *P* values were described in Supplementary Table 3.

A. western blot analysis of AMPK (and its phosphorylation), EGFR (and its phosphorylation), MUC1, and MUC5ac protein expression in the gallbladder of each group mouse. βactin was used as a loading control. Data are representative of three samples for each protein. T172, the activation marker of AMPK phosphorylation at threonine 172; Y1173, the activation marker of EGFR phosphorylation at tyrosine 1173; i.v., $^{AAV2/8}$CAV1 injection (1×10^{11} vg/mice) via i.v. route; i.p., $^{AAV2/8}$CAV1 injection (1×10^{11} vg/mice) via i.p. route; CC, compound c injection (10 mg/kg/day) via i.p. route.

B. qRT-PCR analysis of CCKAR, CHRM2, CHRM3, miR145-5p, MUC1, MUC5ac, and NPC1L1 expression in the gallbladder of each group mouse. 18S rRNA was used as an internal control. Data represent the mean ± SD of three independent experiments. CC, compound c injection (10 mg/kg/day) via i.p. route.

C. The contractile force of gallbladder smooth muscle generated in response to 10 μM acetylcholine or 10 nM cholecystokinin. Data represent the mean ± SD of three independent experiments. Ach, acetylcholine; CCK, cholecystokinin.

D. quantitation of free fatty acids, triacylglycerol, and cholesterol in gallbladder of each group mouse.

Supplementary Files

This is a list of supplementary files associated with this preprint. Click to download.

- SupplementaryFigure1.pdf
- SupplementaryFigure2.pdf
- SupplementaryFigure3.pdf
- SupplementaryTable1.xlsx
- SupplementaryTable2.xlsx
- SupplementaryTable3.xlsx